

Donor-acceptor 1,2,4,5-Tetrazines Prepared by Buchwald-Hartwig Cross-Coupling Reaction and Their Photoluminescence Turn-on Property by Inverse Electron Demand Diels-Alder Reaction

Yangyang Qu,^[a] Piotr Pander,^[b] Oleh Vybornyj,^[c] Marharyta Vasylieva,^[d] Régis Guillot,^[e] Fabien Miomandre,^[a] Fernando B. Dias,^[b] Peter Skabara,^[c] Przemyslaw Data,^[d] Gilles Clavier^[a] and Pierre Audebert*^[a]

^[a] PPSM, CNRS, ENS Paris-Saclay, 61 Avenue Président Wilson, 94235 Cachan, France

^[b] Physics Department, Durham University, South Road, Durham DH1 3LE, UK

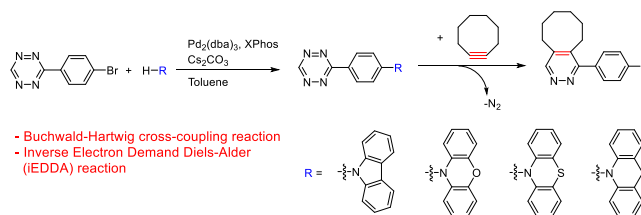
^[c] WestCHEM, School of Chemistry, University of Glasgow, Glasgow G12 8QQ, UK

^[d] Faculty of Chemistry, Silesian University of Technology, M. Stzody 9, 44-100 Gliwice, Poland

^[e] Institut de Chimie Moléculaire et des Matériaux d'Orsay (ICMMO), Université Paris-Sud 11, Université Paris-Saclay, UMR CNRS 8182, Rue du doyen Georges Poitou, 91405 Orsay cedex, France

* E-mail: audebert@ppsm.ens-cachan.fr

Supporting Information Placeholder



ABSTRACT: A facile efficient synthetic tool, Buchwald-Hartwig cross-coupling reaction, for the functionalization of 1,2,4,5-tetrazines is presented. Important factors affecting the Buchwald-Hartwig cross-coupling reaction have been optimized. Seven new donor-acceptor tetrazine molecules (**TA1-TA7**) were conveniently prepared in good to high yields (61%-72%). They have been subsequently engaged in inverse Electron Demand Diels-Alder (IEDDA) reaction with cyclooctyne. The photophysical and electrochemical properties of the new pyridazines have been studied. Some are fluorescent acting as turn-on probes. More importantly two pyridazines (**DA3** and **DA6**) exhibit room temperature phosphorescence (RTP) properties.

INTRODUCTION

The synthesis of 1,2,4,5-tetrazine, or *s*-tetrazine has attracted a significant interest since the inception of fast bioconjugation.^{1,2} Applications spanning biological imaging and detection, cancer targeting, drug delivery and biomaterials science have been recently demonstrated.³⁻¹³ Moreover, for the past several decades electron-deficient 1,2,4,5-tetrazine molecules have been found particularly useful in various fields¹⁴ such as organic electronics (e.g., OPVs, OFETs),¹⁵⁻¹⁷ energetic materials,^{18,19} coordination chemistry,²⁰⁻²² electrofluorochromism²³ and total synthesis of natural products.^{24,25}

The most widely used method for the synthesis of 1,2,4,5-tetrazines is a two-step procedure starting from the addition of hydrazine to nitrile precursors, followed by the oxidation of the resulting 1,2-dihydrotetrazine.¹⁴ In 2012, Devaraj et al. reported a metal-catalyzed one-pot procedure to prepare both symmetrical and unsymmetrical tetrazines from either aromatic or aliphatic nitrile precursors.²⁶ More recently, our group has developed an efficient and metal-free synthetic approach to prepare 3-monosubstituted unsymmetrical 1,2,4,5-tetrazines.²⁷ However, these methods are generally limited in the scope of substrates. The harsh conditions are not compatible with several fragile functional groups such as carbonyls and alkyl halides.⁹

Post-modification on simple tetrazine building blocks has thus been widely used to prepare tetrazines with reactive or complex functional groups, including commonly used fluorophores for bio-imaging application.^{3,14,28} Nucleophilic aromatic substitution (S_NAr) on readily available 1,2,4,5-tetrazine precursors such as 3,6-dichloro-, 3,6-bis(3,5-dimethyl-1*H*-pyrazol-1-yl)- or 3,6-dimethylthio-*s*-tetrazine, has long been regarded as one of the most powerful methods to prepare functionalized

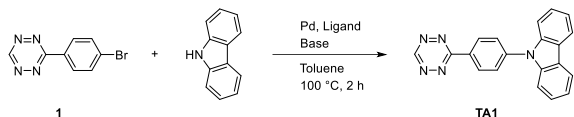
1,2,4,5-tetrazines for various applications.¹⁴ However, to prepare π -conjugated 1,2,4,5-tetrazines, metal-catalyzed cross-coupling reactions on a simple tetrazine precursor are more useful. Although several examples of metal-catalyzed cross-coupling reactions have been reported on tetrazine, most of them still suffer from low yields and limited scope regarding the tetrazine substrates.^{9,29-32} This can be explained by the fact that the nitrogen atoms in the tetrazine ring can act as ligands for a metal and deactivate their catalytic activity or the tetrazine core can be reduced by metals followed by the decomposition of the ring.^{20,33}

Herein we studied an important synthetic tool, Buchwald-Hartwig cross-coupling reaction, for the functionalization of tetrazine compounds. Buchwald-Hartwig cross-coupling reaction is of considerable importance in modern synthetic chemistry, as numerous pharmaceuticals, natural products and novel materials have been synthesized by this methodology.^{34,35} However, there is no detailed study of Buchwald-Hartwig coupling reaction in the tetrazine chemistry to date. The only report describing Buchwald-Hartwig reaction on tetrazine molecules came from our group; however, the scope is limited to only two examples. In addition, the reaction conditions were not optimized and only moderate yields (40% and 47%) were observed after prolonged heating (36 hours and 6 days).³⁶ In this report, we present a systematic study of Buchwald-Hartwig coupling reaction applied to tetrazine molecules, and successfully prepared a series of novel donor-acceptor 1,2,4,5-tetrazine molecules in good to high yields (61%-72%). The important factors influencing the Buchwald-Hartwig cross-coupling reaction for tetrazine functionalization are discussed. Those conditions could be of practical importance for researchers performing Buchwald-Hartwig coupling reaction on other difficult substrates. The methodology provided here not only offers a facile and efficient pathway to prepare new donor-acceptor 1,2,4,5-tetrazine molecules, but is also expected to facilitate the future applications of 1,2,4,5-tetrazines as electron-deficient components in organic electronics and as valuable intermediates for the synthesis of natural products.

RESULTS AND DISCUSSION

We initially chose 3-(4-bromophenyl)-1,2,4,5-tetrazine **1** as the tetrazine substrate, because 3-monosubstituted unsymmetrical tetrazines are useful for bio-orthogonal click chemistry due to their fast cycloaddition reaction rate with strained unsaturated cycloalkanes. Tetrazine **1** was prepared by the metal-free synthetic approach recently developed in our group.²⁷ Molecules with strong electron donating abilities (carbazole, phenoxazine, phenothiazine and 9,10-dihydro-9,9-dimethylacridine) have been chosen for this study, because donor-acceptor molecules are of particular interest in organic electronics, due to the charge transfer (CT) excited states induced by the electron donor-acceptor system.^{37,38} The reaction conditions were optimized by using **1** and carbazole as the starting materials (**Table 1**). Firstly, the choice of base is crucial for the outcome of this reaction. When strong bases such as ^tBuONa ($pK_a = 17$) or lithium hexamethyldisilamide (LHMDS, $pK_a = 26$) were used, the tetrazine precursor **1** quickly degraded resulting in no target product (entries 1 and 2). However, when the weak base NEt_3 ($pK_a = 11$) was chosen, it did not promote the hydrogen bromide elimination, resulting in no reaction at all (entry 5). Fortunately, weak inorganic carbonate bases ($pK_a = 10$) which could react heterogeneously in non-polar solvent were found to promote the hydrogen bromide elimination successfully (entries 3 and 4), and cesium carbonate (CS_2CO_3) was found to be the most reactive resulting in a high yield of the expected product (72%, entry 3). Secondly, the choice of the catalyst and ligand played an important role in the reaction yield. We found out that tris(dibenzylideneacetone)dipalladium(0) ($Pd_2(dba)_3$) was the most effective catalyst tested and 2-dicyclohexylphosphino-2',4',6'-triisopropylbiphenyl (XPhos) gave much better results than other ligands ($P(tBu)_3$, 1,1'-Bis(diphenylphosphino)ferrocene (DPPF), entries 6 and 7).

The optimization of the amount of palladium catalyst and ligand loading is summarized in **Table S1**. It is important to note that excess amount of XPhos relative to $Pd_2(dba)_3$ was necessary to achieve a high yield, and 4 equivalents XPhos to $Pd_2(dba)_3$ was found to give the best yield. This is probably because excess amount of ligand is able to sufficiently stabilize the palladium catalyst and prevents the binding of catalyst to the nitrogen atoms on tetrazine which potentially deactivates the palladium catalyst. The amount of $Pd_2(dba)_3$ and XPhos loading were finally optimized to 3% and 12%, respectively, to give the best yield (72%). Additionally, the influence of the reaction temperature and time was also examined. It was found that both high temperature and a prolonged reaction time are not preferable for this reaction, therefore heating at 100 °C for 2 hours was found to give the best result (**Table S2**).

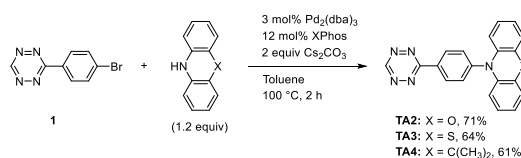
Table 1. Optimization of the reaction conditions^(a).

Entry	Pd, Ligand	Base	Yield (%) ^(b)
1	Pd ₂ (dba) ₃ , Xphos	^t BuONa	0
2	Pd ₂ (dba) ₃ , Xphos	LHMDS	0
3	Pd ₂ (dba) ₃ , Xphos	Cs ₂ CO ₃	72
4	Pd ₂ (dba) ₃ , Xphos	K ₂ CO ₃	35
5	Pd ₂ (dba) ₃ , Xphos	NEt ₃	0
6	Pd ₂ (dba) ₃ , P(^t Bu) ₃	Cs ₂ CO ₃	15
7	Pd ₂ (dba) ₃ , DPPF	Cs ₂ CO ₃	10
8	Pd(OAc) ₂ , Xphos	Cs ₂ CO ₃	56

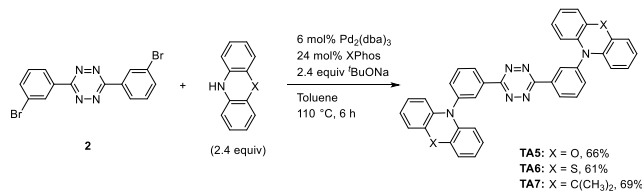
(a) All reactions were carried out on a 0.2 mmol scale in 10 ml of toluene. Pd = palladium catalyst. (b) Yields (isolated) based on the tetrazine precursor **1**.

With these optimized parameters in hand, we intended to extend the scope of this synthetic strategy with other electron rich amines. Three new donor-acceptor 3-monosubstituted unsymmetrical tetrazines **TA2-TA4** were successfully prepared in good to high yields (61%-71%) using phenoxazine, phenothiazine or 9,10-dihydro-9,9-dimethylacridine as a donor instead of carbazole (**Scheme 1**). Moreover, donor-acceptor 3,6-disubstituted symmetrical tetrazines **TA5-TA7** were also prepared in good to high yields (61%-69%) by Buchwald-Hartwig coupling reaction using bifunctional tetrazine precursor **2** (**Scheme 2**). In this case, it was initially found that using the above mentioned optimized conditions only led to a low yield of product (less than 10%), while a large amount of tetrazine precursor **2** was recovered. This suggested that the tetrazine precursor **2** is less reactive than tetrazine **1**, therefore the stronger base ^tBuONa was used to increase the product yields. It was found that tetrazine precursor **2** is more chemically stable to bases compared to tetrazine **1** (tetrazine **2** only degrades slowly in the presence of ^tBuONa), which is important to obtain a high yield of product. As expected, the yield of the reaction significantly increased (up to 69%) using ^tBuONa as a base, along with 6 hours of heating time (necessary to consume tetrazine precursor **2**).

Scheme 1. Synthesis of 3-monosubstituted unsymmetrical tetrazines **TA2-TA4**.



Scheme 2. Synthesis of 3, 6-disubstituted symmetrical tetrazines **TA5-TA7**.



The electrochemical properties and photophysical properties of **TA1-TA7** are depicted in **Table S3** and **Figure S1** and **S3**. Two reversible processes were found for **TA2-7** molecules in cyclic voltammetry, which can be ascribed to the oxidation of the donor moieties and the reduction of the tetrazine acceptor, respectively. The oxidation peak of **TA1** is irreversible because of the carbazole moiety which is known to be irreversibly oxidized (**Figure S3**).^{39,40} The influence of the donor group on the redox potential of the tetrazine is quite insignificant, this being indicative of a weak conjugation in the ground state between these two moieties.

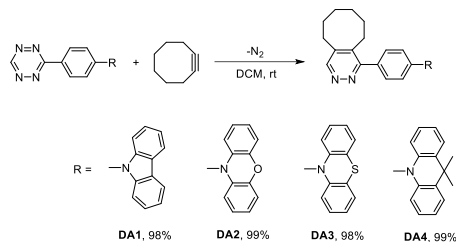
All the **TA** molecules show an absorption band in the visible region with a maximum located near 550 nm and a rather small extinction coefficient (540-700 dm³·mol⁻¹·cm⁻¹), which is typical of the n-π* transition common to all tetrazine derivatives.¹⁴ The second band located around 400 nm is probably the charge transfer one as it has been shown with similar derivatives.^{36,41} In addition, all the **TA** molecules are non-emissive because all the S₁ ¹nπ* molecules transit into the CT triplet state by intersystem crossing according to the El-Sayed's rule, and finally relax non-radiatively to the ground state.^{42,43}

Furthermore, we were interested in applying the inverse Electron Demand Diels-Alder (iEDDA) reaction to the obtained donor-acceptor tetrazine molecules. The Diels-Alder cycloaddition of tetrazines with electron rich dienophiles was first re-

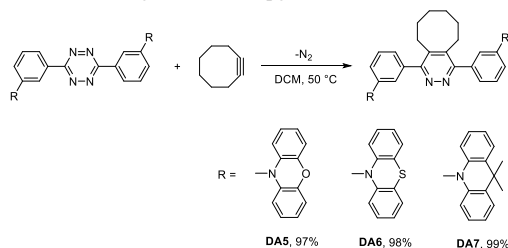
ported in 1959.⁴⁴ Since then, this chemistry has been utilized in a number of studies for preparing biologically active molecules, including a number of studies in total synthesis of natural products,^{24,25,45,46} as well as the recently developed fast bio-conjugation.^{3,4,13}

Cyclooctyne was chosen as the dienophile to react with tetrazine compounds **TA1-TA7**, because the triple bond in cyclooctyne allowed us to obtain the pyridazine products directly in one step without the need for further oxidation and tedious purification steps. In addition, the very fast cycloaddition reaction rate of cyclooctyne with tetrazines⁴⁷ gave molecules **DA1-DA7** in almost quantitative yields (**Scheme 3, 4**). Compounds **TA1-TA4** react with cyclooctyne in dichloromethane (DCM) at room temperature within minutes to give **DA1-DA4**, while the reactions of **TA5-TA7** with cyclooctyne were performed at 50 °C for 1 hour to give **DA5-DA7**. This is in accordance with the reported superior cycloaddition reaction rate of 3-monosubstituted unsymmetrical tetrazines compared to those of 3, 6-disubstituted symmetrical ones.^{3,4}

Scheme 3. Synthesis of pyridazines DA1-DA4.



Scheme 4. Synthesis of pyridazines DA5-DA7.



As mentioned above, all the **TA** molecules are non-emissive; however, photoluminescence appears upon reaction with cyclooctyne in all cases. The reaction of **TA2** with cyclooctyne is exemplified here to show the fluorescence turn-on performance of our donor-acceptor tetrazines (**Figure 1**). After the addition of cyclooctyne, the red color of tetrazine solution quickly disappeared and nitrogen gas evolved, resulting in a colorless and highly cyan emissive solution (**Figure 1c**). The X-ray single crystal structures of both **TA2** and **DA2** are shown in **Figure 1b**. The fluorescence turn-on property was studied by recording fluorescence spectra during the course of the reaction. The gradual increase in emission intensity indicates the formation of the pyridazine moiety (**Figure 2a**). The reaction initially proceeded rapidly (90% conversion of **TA2** to **DA2** in 10 minutes), and completed when it reached a plateau approximately 18 minutes after the addition of cyclooctyne (**Figure 2b**).

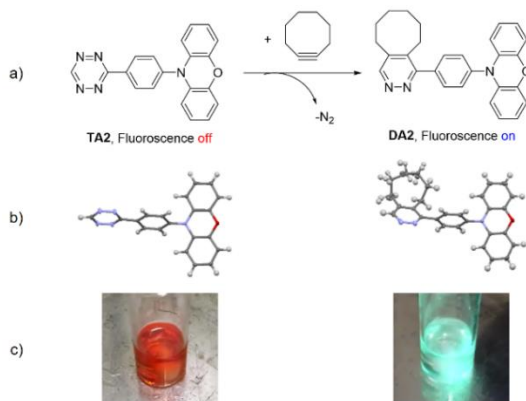


Figure 1. a) iEDDA reaction of **TA2** with cyclooctyne. b) X-ray crystallographic structure of the initial tetrazine (left) and the product (right). c) Photos of the initial compound (left) and the adduct product under 365 nm UV-irradiation (right).

Table 2. Photophysical and electrochemical properties of DA1-DA7.

	λ_{Abs} (nm) ^(a)	λ_{FL} (nm) ^(b)	λ_{Phos} (nm) ^(c)	Φ_{PL} ^(d)	$E_{\text{ox vs Fc/Fc}^+}$ (V) ^(e)	E_{g} (eV) ^(f)	HOMO (eV) ^(g)	LUMO (eV) ^(h)
DA1	238, 292, 326, 340	346, 362	485	< 0.01	0.73	3.52	-5.83	-2.31
DA2	240, 324	536	455, 481	0.15	0.21	3.46	-5.31	-1.85
DA3	258, 314	558	500, 526	0.04	0.21	3.38	-5.31	-1.93
DA4	288	487	488	0.04	0.38	3.32	-5.48	-2.16
DA5	240, 323	577	482	0.02	0.25	3.31	-5.35	-2.04
DA6	258, 317	602	505, 532	0.01	0.29	3.30	-5.39	-2.09
DA7	286	522	478	< 0.01	0.43	3.34	-5.53	-2.19

(a) Absorption maxima recorded in DCM (1×10^{-5} M) at room temperature. (b) Emission maxima recorded in DCM (1×10^{-5} M) at room temperature. (c) Phosphorescence maxima recorded in Zeonex 1% (w/w) at 80 K with a delay of 10 ms after excitation pulse. (d) Photoluminescence quantum yield recorded in DCM at room temperature. (Standard: 9,10-diphenylanthracene in cyclohexane, $\Phi_{\text{PL}} = 0.68$) (e) Onset of the oxidation peak recorded in DCM / 0.1 M Bu_4NPF_6 supporting electrolyte at room temperature by cyclic voltammetry. (f) Optical energy gap in DCM calculated from the onset of the absorption spectra. (g) Highest occupied molecular orbital energy estimated from the onset of the oxidation peak, $E_{\text{HOMO}}/\text{eV} = -(E_{\text{ox}}/V + 5.1)$. (h) Lowest unoccupied molecular orbital energy estimated using optical band gap $E_{\text{LUMO}} = E_{\text{HOMO}} + E_{\text{g}}$.

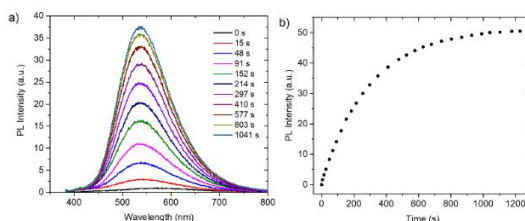


Figure 2. a) Fluorescence spectra recorded during the course of the iEDDA reaction of **TA2** with cyclooctyne in DCM at room temperature. b) Plot of fluorescence intensity (integration of the area of each spectrum) as a function of time.

The electrochemical and photophysical properties of **DA1-DA7** are depicted in **Table 2** and **Figure S2, S4-S11**. Only one redox signal can be found in all **DA** molecules in cyclic voltammetry, corresponding to the oxidation of the donor moiety (**Figure S2**) while the parent **TA** compounds also display the reduction signal of the tetrazine moiety (**Figure S1**). For all **DA** molecules, the reduction signal of the acceptor unit was not observed and it is presumed to lie outside the electrochemical window. The electrochemical behavior of **DA** molecules is very different when comparing the phenoxazine **DA2, DA5** and phenothiazine **DA3, DA6** derivatives on one hand with the carbazole **DA1** and acridine **DA4, DA7** derivatives. The first series show a reversible pure electron transfer with a very slight anodic shift of the oxidation potential for the disubstituted compounds vs. the monosubstituted. Conversely, **DA1, DA4** and **DA7** all display a more complicated response with two successive peaks in forward oxidation and backward reduction. This strongly suggests a radical coupling following the first electron transfer and leading to a dimer or oligomers that precipitate on the electrode surface. Indeed, in absence of heteroatom on the intermediate cycle, the spin density can be delocalized on the terminal positions of the phenyl rings thus favouring the radical coupling. This behavior can also be observed on the parent compounds **TA1, TA4** and **TA7** (see **Figure S1**), the oxidation of **TA1** being even fully irreversible. The disubstituted compound **DA7** behaves similarly to the monosubstituted **DA4** with a very slight anodic shift of its oxidation potential as for the first series. Phenoxazine and phenothiazine substituted **DA2, DA3, DA5** and **DA6** have a lower oxidation potential than the carbazole substituted **DA1** and acridine substituted **DA4** and **DA7** in agreement with the stabilization of the cation radical by the donor effect of the heteroatom.

A clear positive solvatochromic effect was found in fluorescence for **DA2, DA3, DA5** and **DA6** indicating that the emission originates from a charge transfer (CT) excited state (**Figure S6, S7, S9, S10**). However, no such effect could be observed for **DA1, DA4** and **DA7** because these compounds are emissive in DCM but very weakly or not-emissive in other solvents (**Figure S5, S8, S11**). In addition, the phosphorescence spectra of all the **DA** compounds were recorded in Zeonex 1% (w/w) at 80 K at a delay of 10 ms after excitation pulse (**Figure S5-S11**) and data are summarized in **Table 2**.

All the molecules are luminescent to some extent, but most of them remain purely fluorescent. Interestingly, **DA3** and **DA6** exhibit clear room temperature phosphorescence (RTP) properties (**Figure 3** and **Figure S12**) due to an efficient intersystem crossing to a long-lived triplet excited state that is promoted by the phenothiazine donor attached to the pyridazine acceptor core.^{48,49} Phenothiazine (due to the involvement of sulfur's atomic orbitals) not only induces higher triplet formation yield, but also increases radiative decay rate of the triplet state. RTP materials have attracted intensive interests because of their relatively long decay lifetimes and large Stoke shifts, which have already been reported to be useful in many fields such as organic light-emitting diodes (OLEDs),^{50,51} bioimaging and sensing⁵² or organic photovoltaics (OPV).⁵³

The photoluminescence spectrum of **DA3** in Zeonex 1% (w/w) in vacuum shows an additional signal ($\lambda = 500-550$ nm) compared to the spectrum in air-equilibrated condition, which can be attributed to the room temperature phosphorescence (**Figure 3b**). The time-resolved spectra and photoluminescence decay of **DA3** indicate that this additional signal has a long radiative decay lifetime which corresponds to the phosphorescence of the molecule (**Figure 3c, 3d**). The ratio of the room

temperature phosphorescence component to the fluorescence one was determined to be 0.68. In addition, the singlet and triplet energy levels were estimated to be 3.16 eV and 2.63 eV respectively (**Figure 3c**).

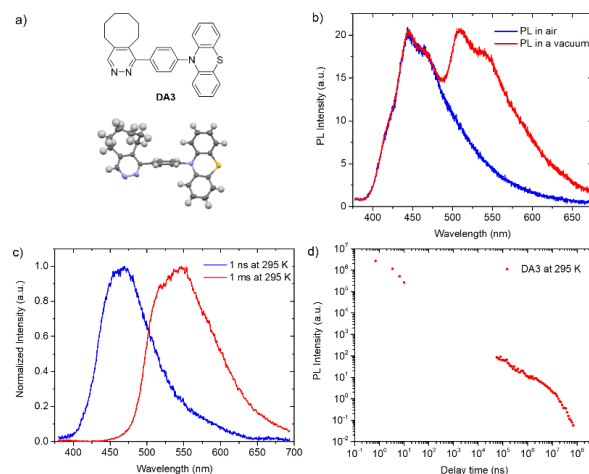


Figure 3. a) Chemical and crystal structure of **DA3**. b) Photoluminescence spectra of **DA3** in Zeonex 1% (w/w) in vacuum (red) and air-equilibrated (blue) conditions at room temperature. c) Time-resolved spectra of **DA3** in Zeonex 1% (w/w) at room temperature in vacuum. The blue spectrum corresponds to the fluorescence and the red one to the phosphorescence. d) PL decays of **DA3** in Zeonex 1% (w/w) at room temperature in vacuum.

In conclusion, we have extended the scope of the Buchwald-Hartwig cross-coupling reaction to the functionalization of 1,2,4,5-tetrazine derivatives. We have shown that this reaction can be used for the preparation of symmetrical and more importantly rather fragile unsymmetrical 3-monosubstituted tetrazines with various electron-rich aromatic secondary amines. This synthetic methodology should largely improve the access to various functionalized 1,2,4,5-tetrazines. Donor-acceptor tetrazine molecules (**TA1-TA7**) were thus conveniently prepared in good to high yields (61%-72%) which were shown to act as new tetrazine turn-on luminescent probes by iEDDA reaction with cyclooctyne. Moreover, the cycloaddition products pyridazines **DA3** and **DA6** have been found to exhibit promising RTP properties.

EXPERIMENTAL SECTION

General Methods. All chemicals were received from commercial sources and used without further purification. Thin layer chromatography (TLC) was performed on silica gel. Flash column chromatography purification was performed on a CombiFlash-Rf system with a variable wavelength UV detector. All mixtures of solvents are given in v/v ratio. NMR spectra were recorded on a JEOL ECS (400 MHz) spectrometer. ^{13}C NMR spectra were proton decoupled. HRMS spectra were measured either on an UPLC/ESI-HRMS device (an Acquity Waters UPLC system coupled to a Waters LCT Premier XE mass spectrometer equipped with an electrospray ion source), or a Q-TOF mass spectrometer (Q-TOF 6540, Agilent) equipped with an APPI ion source. Melting points (m.p.) were determined on a Reichert Kofler Heizbank melting point apparatus and a KRÜSS melting point meter M5000.

Tetrazine **1**,²⁷ **2A1** and cyclooctyne⁵⁴ were prepared according to published procedures.

X-ray diffraction data for compounds **TA2**, **TA3**, **DA2** and **DA3** were collected by using a VENTURE PHOTON100 CMOS Bruker diffractometer with Micro-focus IuS source Mo $\text{K}\alpha$ radiation. Crystal was mounted on a CryoLoop (Hampton Research) with Paratone-N (Hampton Research) as cryoprotectant and then flashfrozen in a nitrogen-gas stream at 100 or 250 K. The temperature of the crystal was maintained at the selected value by means of an N-Helix to within an accuracy of $\pm 1\text{K}$. The data were corrected for Lorentz polarization, and absorption effects. The structures were solved by direct methods using SHELXS-97⁵⁵ and refined against F^2 by full-matrix least-squares techniques using SHELXL-2018⁵⁶ with anisotropic displacement parameters for all non-hydrogen atoms. All calculations were performed by using the Crystal Structure crystallographic software package WINGX.⁵⁷

The crystal data collection and refinement parameters are given in **Table S4**. ORTEP drawing of the compounds are shown in **Figure S13-S16**.

CCDC 1937098-1937101 contains the supplementary crystallographic data for this paper. These data can be obtained free of charge from the Cambridge Crystallographic Data Centre via <http://www.ccdc.cam.ac.uk/Community/Requeststructure>.

Photophysics. Zeonex @ 480 blends were prepared from toluene solutions by the drop-cast method and dried in a vacuum (Zeonex @ 480 is a type of Cyclo Olefin Polymer (COP) developed by ZEON CORPORATION). All solutions were investigated at 10^{-5} mol dm^{-3} concentration and were degassed using five freeze/pump cycles. Absorption and emission spectra were collected using a UV-3600 double beam spectrophotometer (Shimadzu), and a Fluoromax fluorescence spectrometer (Jobin Yvon) or QePro fluorescence spectrometer (Ocean Optics). Photoluminescence quantum yields in DCM solution were measured using 9,10-diphenylanthracene in cyclohexane ($\Phi_{\text{PL}} = 0.68$) as the standard.

Phosphorescence and prompt fluorescence (PF) spectra and decays were recorded using nanosecond gated luminescence and lifetime measurements (from 400 ps to 1 s) using either third harmonics of a high-energy, pulsed Nd:YAG laser emitting at 355 nm (EKSPILA) or a N2 laser emitting at 337 nm. Emission was focused onto a spectrograph and detected on a sensitive gated iCCD camera (Stanford Computer Optics) of sub-nanosecond resolution. PF/DF time-resolved measurements were performed by exponentially increasing gate and delay times.

Electrochemistry. The electrochemical cell comprised of platinum electrode with a 1 mm diameter of working area as a working electrode, an Ag electrode as a reference electrode and a platinum coil as an auxiliary electrode. Cyclic voltammetry measurements were conducted at room temperature at a potential rate of 50 mV/s and were calibrated against ferrocene/ferrocenium redox couple. All voltammograms were recorded on a CHInstruments Electrochemical Analyzer model 660 potentiostat. Electrochemical measurements were conducted in 1.0 mM concentrations for all cyclic voltammetry measurements. Electrochemical studies were undertaken in 0.1 M solutions of Bu₄NPF₆, 99% in dichloromethane (DCM) at room temperature.

Synthesis.

9-(4-(1,2,4,5-tetrazin-3-yl)phenyl)-9H-carbazole (TA1)

Procedure A: To a 100 ml two-neck round bottom flask equipped with a stir bar, tetrazine **1** (0.2 mmol, 47.6 mg), carbazole donor (0.24 mmol, 40.1 mg), cesium carbonate (0.4 mmol, 130 mg) and 10 ml of anhydrous toluene were added. The reaction mixture was degassed by bubbling through nitrogen for 15 min under vigorous stirring. Then Pd₂(dba)₃ (0.006 mmol, 5.5 mg) and XPhos (0.024 mmol, 11.5 mg) were added and degassed for another 15 min. The reaction mixture was heated to 100 °C on a heat-on reaction block under a nitrogen atmosphere and stirred for 2 h. The reaction mixture was then cooled down to room temperature, extracted with dichloromethane. The organic phase was dried over anhydrous magnesium sulfate (MgSO₄), filtered and concentrated under reduced pressure. The product was purified using flash column chromatography (Petroleum ether:CH₂Cl₂ = 3:1) to give 46.5 mg of **TA1** as a red solid (yield: 72%). ¹H NMR (400 MHz, CDCl₃, δ): 10.27 (s, 1H), 8.89 (d, *J* = 8.24 Hz, 2H), 8.17 (d, *J* = 7.80 Hz, 2H), 7.88 (d, *J* = 8.24 Hz, 2H), 7.56 (d, *J* = 7.80 Hz, 2H), 7.46 (t, *J* = 7.80 Hz, 2H), 7.34 (t, *J* = 7.80 Hz, 2H) ppm; ¹³C{¹H} NMR (100 MHz, CDCl₃, δ): 166.1, 158.0, 142.6, 140.3, 130.10, 130.06, 127.4, 126.4, 124.1, 120.8, 120.7, 110.0 ppm; HRMS [M+H]⁺ *m/z* calcd. for [C₂₀H₁₄N₅]⁺ 324.1249, found 324.1253; m.p. 180 °C.

10-(4-(1,2,4,5-tetrazin-3-yl)phenyl)-10H-phenoxazine (TA2)

TA2 was prepared following **Procedure A** using phenoxazine as a donor. A deep red solid was obtained after flash column chromatography (Petroleum ether:CH₂Cl₂ = 3:1) (48.1 mg, yield: 71%). Single crystal of **TA2** was grown from slow evaporation of petroleum ether/CH₂Cl₂ (3:1) mixture. ¹H NMR (400 MHz, CDCl₃, δ): 10.28 (s, 1H), 8.87 (d, *J* = 8.24 Hz, 2H), 7.63 (d, *J* = 8.24 Hz, 2H), 6.79–6.59 (m, 6H), 6.05 (dd, *J* = 7.80 Hz, *J* = 1.50 Hz, 2H) ppm; ¹³C{¹H} NMR (100 MHz, CDCl₃, δ): 166.1, 158.0, 144.2, 144.1, 133.8, 132.0, 131.6, 131.2, 123.5, 122.1, 115.9, 113.5 ppm; HRMS [M+H]⁺ *m/z* calcd. for [C₂₀H₁₄N₅O]⁺ 340.1198, found 340.1192; m.p. 243 °C.

10-(4-(1,2,4,5-tetrazin-3-yl)phenyl)-10H-phenothiazine (TA3)

TA3 was prepared following **Procedure A** using phenothiazine as a donor. A deep red solid was obtained after flash column chromatography (Petroleum ether:CH₂Cl₂ = 3:1) (45.4 mg, yield: 64%). Single crystal of **TA3** was grown from slow evaporation of petroleum ether/CH₂Cl₂ (3:1) mixture. ¹H NMR (400 MHz, CDCl₃, δ): 10.13 (s, 1H), 8.56 (d, *J* = 8.24 Hz, 2H), 7.37 (d, *J* = 7.80 Hz, 2H), 7.32 (d, *J* = 8.24 Hz, 2H), 7.24 (d, *J* = 7.80 Hz, 2H), 7.17–7.10 (m, 4H) ppm; ¹³C{¹H} NMR (100 MHz, CDCl₃, δ): 166.2, 157.5, 148.9, 141.9, 130.7, 130.2, 128.6, 127.4, 125.8, 125.6, 124.1, 120.1 ppm; HRMS [M+H]⁺ *m/z* calcd. for [C₂₀H₁₄N₅S]⁺ 356.0970, found 356.0977.

10-(4-(1,2,4,5-tetrazin-3-yl)phenyl)-9,9-dimethyl-9,10-dihydroacridine (TA4)

TA4 was prepared following **Procedure A** using 9,10-dihydro-9,9-dimethylacridine as a donor. A red solid was obtained after flash column chromatography (Petroleum ether:CH₂Cl₂ = 3:1) (44.4 mg, yield: 61%). ¹H NMR (400 MHz, CDCl₃, δ): 10.28 (s, 1H), 8.89 (d, *J* = 8.24 Hz, 2H), 7.62 (d, *J* = 8.24 Hz, 2H), 7.49 (dd, *J* = 7.80 Hz, *J* = 1.80 Hz, 2H), 7.05–6.95 (m, 4H), 6.40 (dd, *J* = 7.80 Hz, *J* = 1.80 Hz, 2H) ppm; ¹³C{¹H} NMR (100 MHz, CDCl₃, δ): 166.2, 158.0, 146.4, 140.6, 131.9, 131.1, 131.0, 126.6, 125.5, 121.4, 114.6, 36.3, 31.2 ppm; HRMS [M+H]⁺ *m/z* calcd. for [C₂₃H₂₀N₅]⁺ 366.1719, found 366.1725.

3,6-bis(3-(10H-phenoxazin-10-yl)phenyl)-1,2,4,5-tetrazine (TA5)

Procedure B: To a 100 ml two-neck round bottom flask equipped with a stir bar, tetrazine **2** (0.2 mmol, 78.4 mg), phenoxazine donor (0.48 mmol, 87.9 mg), sodium *tert*-butoxide (0.48 mmol, 46.1 mg) and 15 ml of anhydrous toluene were added. The reaction mixture was degassed by bubbling through nitrogen for 15 min under vigorous stirring. Then Pd₂(dba)₃ (0.012 mmol, 11 mg) and XPhos (0.048 mmol, 23 mg) were added and degassed for another 15 min. The reaction mixture was heated to 110 °C on a heat-on reaction block under a nitrogen atmosphere and stirred for 6 h. The reaction mixture was then cooled down to room temperature, extracted with dichloromethane. The organic phase was dried over anhydrous magnesium sulfate (MgSO₄), filtered and concentrated under reduced pressure. The product was purified using flash column chromatography (Petroleum ether:CH₂Cl₂ = 4:1) to give 78.3 mg of **TA5** as a purple solid (yield: 66%). ¹H NMR (400 MHz, CDCl₃, δ): 8.77 (d, *J* =

8.24 Hz, 2H), 8.69 (t, $J = 1.80$ Hz, 2H), 7.87 (t, $J = 8.24$ Hz, 2H), 7.67 (d, $J = 8.24$ Hz, 2H), 6.77–6.56 (m, 12H), 6.00 (dd, $J = 7.80$ Hz, $J = 1.80$ Hz, 4H) ppm; $^{13}\text{C}\{^1\text{H}\}$ NMR (100 MHz, CDCl_3 , δ): 163.6, 144.1, 140.6, 135.8, 135.0, 134.1, 132.4, 131.1, 128.2, 123.5, 121.9, 115.8, 113.4 ppm; HRMS $[\text{M}]^+$ m/z calcd. for $[\text{C}_{38}\text{H}_{24}\text{N}_6\text{O}_2]^+$ 596.1961, found 596.1947; m.p. >260 °C.

3,6-bis(3-(10H-phenothiazin-10-yl)phenyl)-1,2,4,5-tetrazine (TA6)

TA6 was prepared following **Procedure B** using phenothiazine as a donor. A red solid was obtained after flash column chromatography (Petroleum ether: $\text{CH}_2\text{Cl}_2 = 4:1$) (76.3 mg, yield: 61%). ^1H NMR (400 MHz, CDCl_3 , δ): 8.74–8.67 (m, 4H), 7.81 (t, $J = 8.24$ Hz, 2H), 7.66 (d, $J = 8.24$ Hz, 2H), 7.11 (dd, $J = 7.80$ Hz, $J = 1.80$ Hz, 4H), 6.97–6.85 (m, 8H), 6.44 (dd, $J = 7.80$ Hz, $J = 1.80$ Hz, 4H) ppm; $^{13}\text{C}\{^1\text{H}\}$ NMR (100 MHz, CDCl_3 , δ): 163.7, 143.8, 143.0, 134.5, 134.0, 131.8, 129.1, 127.3, 127.2, 127.1, 123.4, 122.4, 117.6 ppm; HRMS $[\text{M}]^+$ m/z calcd. for $[\text{C}_{38}\text{H}_{24}\text{N}_6\text{S}_2]^+$ 628.1504, found 628.1500; m.p. >260 °C.

3,6-bis(3-(9,9-dimethylacridin-10(9H)-yl)phenyl)-1,2,4,5-tetrazine (TA7)

TA7 was prepared following **Procedure B** using 9,10-dihydro-9,9-dimethylacridine as a donor. A red solid was obtained after flash column chromatography (Petroleum ether: $\text{CH}_2\text{Cl}_2 = 4:1$) (89.9 mg, yield: 69%). ^1H NMR (400 MHz, CDCl_3 , δ): 8.81 (d, $J = 8.24$ Hz, 2H), 8.67 (t, $J = 1.80$ Hz, 2H), 7.90 (t, $J = 8.24$ Hz, 2H), 7.66 (d, $J = 8.24$ Hz, 2H), 7.49 (dd, $J = 7.80$ Hz, $J = 1.80$ Hz, 4H), 7.03–6.91 (m, 8H), 6.34 (dd, $J = 7.80$ Hz, $J = 1.80$ Hz, 4H), 1.72 (s, 12H) ppm; $^{13}\text{C}\{^1\text{H}\}$ NMR (100 MHz, CDCl_3 , δ): 163.7, 142.6, 140.8, 136.4, 134.9, 132.1, 131.4, 130.4, 127.9, 126.6, 125.5, 121.0, 114.1, 36.2, 31.3 ppm; HRMS $[\text{M}+\text{H}]^+$ m/z calcd. for $[\text{C}_{44}\text{H}_{37}\text{N}_6]^+$ 649.3080, found 649.3093; m.p. >260 °C.

Procedure for synthesis of DA1-DA4

To a 50 mL round bottom flask equipped with a stir bar, 0.1 mmol of **TA1-TA4**, and 10 mL of DCM were added. Then 4 equivalents of cyclooctyne (50 μL) was added with stirring at room temperature. The color of the solution turned from red to colorless after several minutes and N_2 gas evolved. The reaction mixture was allowed to stir for another 20 min. All the volatiles were evaporated under vacuum and the residue was purified using flash column chromatography.

9-(4-(5,6,7,8,9,10-hexahydrocycloocta[d]pyridazin-1-yl)phenyl)-9H-carbazole (DA1)

A white solid was obtained after flash column chromatography (Petroleum ether:EtOAc = 2:3) (39.6 mg, yield: 98%). ^1H NMR (400 MHz, CDCl_3 , δ): 8.96 (s, 1H), 8.17 (d, $J = 8.24$ Hz, 2H), 7.78–7.68 (m, 4H), 7.51 (d, $J = 7.80$ Hz, 2H), 7.44 (t, $J = 7.80$ Hz, 2H), 7.32 (t, $J = 7.80$ Hz, 2H), 2.94–2.85 (m, 4H), 1.90–1.80 (m, 2H), 1.76–1.66 (m, 2H), 1.54–1.40 (m, 4H) ppm; $^{13}\text{C}\{^1\text{H}\}$ NMR (100 MHz, CDCl_3 , δ): 161.3, 151.8, 141.6, 140.8, 138.9, 138.3, 137.0, 130.8, 126.9, 126.2, 123.7, 120.5, 120.3, 109.9, 31.3, 30.6, 29.7, 26.8, 26.1, 25.6 ppm; HRMS $[\text{M}+\text{H}]^+$ m/z calcd. for $[\text{C}_{28}\text{H}_{26}\text{N}_3]^+$ 404.2127, found 404.2127; m.p. 251 °C (dec.).

10-(4-(5,6,7,8,9,10-hexahydrocycloocta[d]pyridazin-1-yl)phenyl)-10H-phenoxazine (DA2)

A white solid was obtained after flash column chromatography (Petroleum ether:EtOAc = 2:3) (41.5 mg, yield: 99%). Single crystal of **DA2** was grown from slow evaporation of petroleum ether/EtOAc (2:3) mixture. ^1H NMR (400 MHz, CDCl_3 , δ): 8.97 (s, 1H), 7.73 (d, $J = 8.24$ Hz, 2H), 7.48 (d, $J = 8.24$ Hz, 2H), 6.76–6.57 (m, 6H), 6.01 (d, $J = 7.80$ Hz, 2H), 2.95–2.81 (m, 4H), 1.89–1.79 (m, 2H), 1.71–1.61 (m, 2H), 1.55–1.38 (m, 4H) ppm; $^{13}\text{C}\{^1\text{H}\}$ NMR (100 MHz, CDCl_3 , δ): 161.3, 151.3, 144.1, 142.2, 139.7, 139.6, 137.8, 134.3, 132.0, 131.0, 123.4, 121.7, 115.7, 113.5, 31.3, 30.5, 29.8, 26.9, 26.1, 25.5 ppm; HRMS $[\text{M}+\text{H}]^+$ m/z calcd. for $[\text{C}_{28}\text{H}_{26}\text{N}_3\text{O}]^+$ 420.2076, found 420.2090; m.p. 182 °C.

10-(4-(5,6,7,8,9,10-hexahydrocycloocta[d]pyridazin-1-yl)phenyl)-10H-phenothiazine (DA3)

A light yellow solid was obtained after flash column chromatography (Petroleum ether:EtOAc = 2:3) (42.6 mg, yield: 98%). Single crystal of **DA3** was grown from slow evaporation of petroleum ether/EtOAc (2:3) mixture. ^1H NMR (400 MHz, CDCl_3 , δ): 8.94 (s, 1H), 7.71 (d, $J = 8.24$ Hz, 2H), 7.49 (d, $J = 8.24$ Hz, 2H), 7.07 (d, $J = 7.80$ Hz, 2H), 6.96–6.82 (m, 4H), 6.38 (d, $J = 7.80$ Hz, 2H), 2.93–2.81 (m, 4H), 1.89–1.78 (m, 2H), 1.71–1.61 (m, 2H), 1.54–1.38 (m, 4H) ppm; $^{13}\text{C}\{^1\text{H}\}$ NMR (100 MHz, CDCl_3 , δ): 161.3, 151.7, 144.1, 141.9, 141.5, 138.8, 137.4, 131.6, 129.9, 127.08, 127.05, 123.0, 121.5, 117.1, 31.3, 30.5, 29.7, 26.8, 26.1, 25.6 ppm; HRMS $[\text{M}+\text{H}]^+$ m/z calcd. for $[\text{C}_{28}\text{H}_{26}\text{N}_3\text{S}]^+$ 436.1847, found 436.1855; m.p. 204 °C.

10-(4-(5,6,7,8,9,10-hexahydrocycloocta[d]pyridazin-1-yl)phenyl)-9,9-dimethyl-9,10-dihydroacridine (DA4)

A white solid was obtained after flash column chromatography (Petroleum ether:EtOAc = 2:3) (44.1 mg, yield: 99%). ^1H NMR (400 MHz, CDCl_3 , δ): 8.97 (s, 1H), 7.77 (d, $J = 8.24$ Hz, 2H), 7.54–7.44 (m, 4H), 7.05–6.91 (m, 4H), 6.37 (d, $J = 7.80$ Hz, 2H), 2.94–2.84 (m, 4H), 1.89–1.80 (m, 2H), 1.71 (s, 6H), 1.71–1.65 (m, 2H), 1.55–1.40 (m, 4H) ppm; $^{13}\text{C}\{^1\text{H}\}$ NMR (100 MHz, CDCl_3 , δ): 161.3, 151.8, 141.7, 141.5, 140.9, 138.8, 137.9, 131.8, 131.4, 130.2, 126.5, 125.4, 120.8, 114.2, 36.1, 31.3, 31.2, 30.4, 29.7, 26.8, 26.1, 25.5 ppm; HRMS $[\text{M}+\text{H}]^+$ m/z calcd. for $[\text{C}_{31}\text{H}_{32}\text{N}_3]^+$ 446.2596, found 446.2606; m.p. 194 °C.

Procedure for synthesis of DA5-DA7

To a 50 mL round bottom flask equipped with a stir bar, 0.1 mmol of **TA5-TA7**, and 15 mL of DCM were added. Then 4 equivalents of cyclooctyne (50 μ L) was added with stirring at room temperature. The reaction mixture was heated to 50 °C on a heat-on reaction block and allowed to stir for 1 hour. The color of the solution turned from red to colorless indicating the completion of the reaction. The reaction mixture was then cooled down to room temperature. All the volatiles were evaporated under vacuum and the residue was purified using flash column chromatography.

1,4-bis(3-(10H-phenoxazin-10-yl)phenyl)-5,6,7,8,9,10-hexahydrocycloocta[d]pyridazine (DA5)

A light yellow solid was obtained after flash column chromatography (Petroleum ether:EtOAc = 2:1) (65.8 mg, yield: 97%). ^1H NMR (400 MHz, CDCl_3 , δ): 7.75 (t, J = 8.24 Hz, 2H), 7.66 (d, J = 8.24 Hz, 2H), 7.52 (s, 2H), 7.48 (d, J = 8.24 Hz, 2H), 6.74–6.56 (m, 12H), 6.03 (d, J = 7.80 Hz, 4H), 2.84 (s, br, 4H), 1.60 (s, br, 4H), 1.41 (s, br, 4H) ppm; $^{13}\text{C}\{^1\text{H}\}$ NMR (100 MHz, CDCl_3 , δ): 160.4, 144.0, 141.0, 139.7, 139.0, 134.3, 131.7, 131.5, 131.2, 129.6, 123.4, 121.6, 115.6, 113.4, 30.4, 27.5, 25.9 ppm; HRMS $[\text{M}+\text{H}]^+$ m/z calcd. for $[\text{C}_{46}\text{H}_{37}\text{N}_4\text{O}_2]^+$ 677.2917, found 677.2923; m.p. >260 °C.

1,4-bis(3-(10H-phenothiazin-10-yl)phenyl)-5,6,7,8,9,10-hexahydrocycloocta[d]pyridazine (DA6)

A light yellow solid was obtained after flash column chromatography (Petroleum ether:EtOAc = 2:1) (69.3 mg, yield: 98%). ^1H NMR (400 MHz, CDCl_3 , δ): 7.73 (t, J = 8.24 Hz, 2H), 7.63 (d, J = 8.24 Hz, 2H), 7.54 (s, 2H), 7.51 (d, J = 8.24 Hz, 2H), 7.04 (dd, J = 7.80 Hz, J = 1.80 Hz, 4H), 6.93–6.79 (m, 8H), 6.36 (d, J = 7.80 Hz, 4H), 2.85 (s, br, 4H), 1.60 (s, br, 4H), 1.40 (s, br, 4H) ppm; $^{13}\text{C}\{^1\text{H}\}$ NMR (100 MHz, CDCl_3 , δ): 160.5, 144.1, 141.3, 140.6, 139.7, 131.2, 131.0, 130.4, 128.9, 127.1, 127.0, 122.9, 121.0, 116.8, 30.4, 27.5, 25.9 ppm; HRMS $[\text{M}+\text{H}]^+$ m/z calcd. for $[\text{C}_{46}\text{H}_{37}\text{N}_4\text{S}_2]^+$ 709.2460, found 709.2485; m.p. 250 °C.

1,4-bis(3-(9,9-dimethylacridin-10(9H)-yl)phenyl)-5,6,7,8,9,10-hexahydrocycloocta[d]pyridazine (DA7)

A white solid was obtained after flash column chromatography (Petroleum ether:EtOAc = 2:1) (72.1 mg, yield: 99%). ^1H NMR (400 MHz, CDCl_3 , δ): 7.78 (t, J = 8.24 Hz, 2H), 7.70 (d, J = 8.24 Hz, 2H), 7.52 (t, J = 1.80 Hz, 2H), 7.50–7.43 (m, 6H), 7.03–6.90 (m, 8H), 6.39 (d, J = 7.80 Hz, J = 1.80 Hz, 4H), 2.94–2.82 (m, 4H), 1.70 (s, 12H), 1.60 (s, br, 4H), 1.38 (s, br, 4H) ppm; $^{13}\text{C}\{^1\text{H}\}$ NMR (100 MHz, CDCl_3 , δ): 160.5, 141.2, 141.02, 140.99, 139.4, 132.2, 131.6, 131.3, 130.2, 129.3, 126.6, 125.3, 120.8, 114.2, 36.1, 31.3, 30.3, 27.5, 25.9 ppm; HRMS $[\text{M}+\text{H}]^+$ m/z calcd. for $[\text{C}_{52}\text{H}_{49}\text{N}_4]^+$ 729.3957, found 729.3975; m.p. 221 °C.

ASSOCIATED CONTENT

Supporting Information

The Supporting Information is available free of charge on the ACS Publications website.

Supporting data for optimization of reaction conditions; supporting photophysical and electrochemical data and spectra; crystallographic data and ORTEP drawings of TA2, TA3, DA2 and DA3; ^1H and ^{13}C NMR spectra of all reported compounds found in the SI.

AUTHOR INFORMATION

Corresponding Author

* E-mail: audebert@ppsm.ens-cachan.fr

Author Contributions

The manuscript was written through contributions of all authors.

Notes

Any additional relevant notes should be placed here.

ACKNOWLEDGMENT

The research leading to these results has received funding from the European Union's Horizon 2020 research and innovation programme under the Marie Skłodowska-Curie grant agreement No 674990 (EXCILIGHT).

REFERENCES

- Blackman, M. L.; Royzen, M.; Fox, J. M. Tetrazine Ligation: Fast Bioconjugation Based on Inverse-Electron-Demand Diels–Alder Reactivity. *J. Am. Chem. Soc.* **2008**, *130* (41), 13518–13519.
- Devaraj, N. K.; Weissleder, R.; Hilderbrand, S. A. Tetrazine-Based Cycloadditions: Application to Pretargeted Live Cell Imaging. *Bioconjug. Chem.* **2008**, *19* (12), 2297–2299.
- Oliveira, B. L.; Guo, Z.; Bernardes, G. J. L. Inverse Electron Demand Diels–Alder Reactions in Chemical Biology. *Chem. Soc. Rev.* **2017**, *46* (16), 4895–4950.
- Knall, A. C.; Slugovc, C. Inverse Electron Demand Diels–Alder (IEDDA)-Initiated Conjugation: A (High) Potential Click Chemistry Scheme. *Chem. Soc. Rev.* **2013**, *42* (12), 5131–5142.
- He, T.; Ren, C.; Luo, Y.; Wang, Q.; Li, J.; Lin, X.; Ye, C.; Hu, W.; Zhang, J. Water-Soluble Chiral Tetrazine Derivatives: Towards the Application of Circularly Polarized Luminescence from Upper-Excited States to Photodynamic Therapy. *Chem. Sci.* **2019**, *10* (15), 4163–4168.
- Lang, K.; Davis, L.; Torres-Kolbus, J.; Chou, C.; Deiters, A.; Chin, J. W. Genetically Encoded Norbornene Directs Site-Specific Cellular Protein Labelling via a Rapid Bioorthogonal Reaction. *Nat. Chem.* **2012**, *4* (4), 298–304.

- (7) Carlson, J. C. T.; Meimetis, L. G.; Hilderbrand, S. A.; Weissleder, R. BODIPY-Tetrazine Derivatives as Superbright Bioorthogonal Turn-on Probes. *Angew. Chem. Int. Ed.* **2013**, *52* (27), 6917–6920.
- (8) Meimetis, L. G.; Carlson, J. C. T.; Giedt, R. J.; Kohler, R. H.; Weissleder, R. Ultrafluorogenic Coumarin–Tetrazine Probes for Real-Time Biological Imaging. *Angew. Chem. Int. Ed.* **2014**, *53* (29), 7531–7534.
- (9) Wu, H.; Yang, J.; Seckute, J.; Devaraj, N. K. In Situ Synthesis of Alkenyl Tetrazines for Highly Fluorogenic Bioorthogonal Live-Cell Imaging Probes. *Angew. Chem. Int. Ed.* **2014**, *53* (23), 5805–5809.
- (10) Uttamapinant, C.; Howe, J. D.; Lang, K.; Beránek, V.; Davis, L.; Mahesh, M.; Barry, N. P.; Chin, J. W. Genetic Code Expansion Enables Live-Cell and Super-Resolution Imaging of Site-Specifically Labeled Cellular Proteins. *J. Am. Chem. Soc.* **2015**, *137* (14), 4602–4605.
- (11) Jiménez-Moreno, E.; Guo, Z.; Oliveira, B. L.; Albuquerque, I. S.; Kitowski, A.; Guerreiro, A.; Boutureira, O.; Rodrigues, T.; Jiménez-Osés, G.; Bernardes, G. J. L. Vinyl Ether/Tetrazine Pair for the Traceless Release of Alcohols in Cells. *Angew. Chem. Int. Ed.* **2017**, *56* (1), 243–247.
- (12) Lee, Y.; Cho, W.; Sung, J.; Kim, E.; Park, S. B. Monochromophoric Design Strategy for Tetrazine-Based Colorful Bioorthogonal Probes with a Single Fluorescent Core Skeleton. *J. Am. Chem. Soc.* **2018**, *140* (3), 974–983.
- (13) Wu, H.; Devaraj, N. K. Inverse Electron-Demand Diels–Alder Bioorthogonal Reactions. *Top. Curr. Chem.* **2016**, *374*, 3.
- (14) Clavier, G.; Audebert, P. S-Tetrazines as Building Blocks for New Functional Molecules and Molecular Materials. *Chem. Rev.* **2010**, *110* (6), 3299–3314.
- (15) Li, Z.; Ding, J.; Song, N.; Lu, J.; Tao, Y. Development of a New S-Tetrazine-Based Copolymer for Efficient Solar Cells. *J. Am. Chem. Soc.* **2010**, *132* (38), 13160–13161.
- (16) Li, Z.; Ding, J.; Song, N.; Du, X.; Zhou, J.; Lu, J.; Tao, Y. Alternating Copolymers of Dithienyl-s-Tetrazine and Cyclopentadithiophene for Organic Photovoltaic Applications. *Chem. Mater.* **2011**, *23* (7), 1977–1984.
- (17) Hwang, D. K.; Dasari, R. R.; Fenoll, M.; Alain-Rizzo, V.; Dindar, A.; Shim, J. W.; Deb, N.; Fuentes-Hernandez, C.; Barlow, S.; Bucknall, D. G.; et al. Stable Solution-Processed Molecular n-Channel Organic Field-Effect Transistors. *Adv. Mater.* **2012**, *24* (32), 4445–4450.
- (18) Huynh, M. H. V.; Hiskey, M. A.; Chavez, D. E.; Naud, D. L.; Gilardi, R. D. Synthesis, Characterization, and Energetic Properties of Diazido Heteroaromatic High-Nitrogen C–N Compound. *J. Am. Chem. Soc.* **2005**, *127* (36), 12537–12543.
- (19) Chavez, D. E.; Parrish, D. A.; Mitchell, L.; Imler, G. H. Azido and Tetrazolo 1,2,4,5-Tetrazine N-Oxides. *Angew. Chem. Int. Ed.* **2017**, *56* (13), 3575–3578.
- (20) Kaim, W. The Coordination Chemistry of 1,2,4,5-Tetrazines. *Coord. Chem. Rev.* **2002**, *230* (1), 127–139.
- (21) Tang, T. S. M.; Liu, H. W.; Lo, K. K. W. Monochromophoric Iridium(III) Pyridyl-Tetrazine Complexes as a Unique Design Strategy for Bioorthogonal Probes with Luminogenic Behavior. *Chem. Commun.* **2017**, *53* (23), 3299–3302.
- (22) Yuasa, J.; Mitsui, A.; Kawai, T. π - π^* Emission from a Tetrazine Derivative Complexed with Zinc Ion in Aqueous Solution: A Unique Water-Soluble Fluorophore. *Chem. Commun.* **2011**, *47* (20), 5807–5809.
- (23) Audebert, P.; Miomandre, F. Electrofluorochromism: From Molecular Systems to Set-up and Display. *Chem. Sci.* **2013**, *4* (2), 575–584.
- (24) Hamasaki, A.; Zimpleman, J. M.; Hwang, I.; Boger, D. L. Total Synthesis of Ningalin D. *J. Am. Chem. Soc.* **2005**, *127* (30), 10767–10770.
- (25) Boger, D. L.; Hong, J. Asymmetric Total Synthesis of Ent-(–)-Roseophilin: Assignment of Absolute Configuration. *J. Am. Chem. Soc.* **2001**, *123* (35), 8515–8519.
- (26) Yang, J.; Karver, M. R.; Li, W.; Sahu, S.; Devaraj, N. K. Metal-Catalyzed One-Pot Synthesis of Tetrazines Directly from Aliphatic Nitriles and Hydrazine. *Angew. Chem. Int. Ed.* **2012**, *51* (21), 5222–5225.
- (27) Qu, Y.; Sauvage, F.-X.; Clavier, G.; Miomandre, F.; Audebert, P. Metal-Free Synthetic Approach to 3-Monosubstituted Unsymmetrical 1,2,4,5-Tetrazines Useful for Bioorthogonal Reactions. *Angew. Chem. Int. Ed.* **2018**, *57* (37), 12057–12061.
- (28) Wu, H.; Devaraj, N. K. Advances in Tetrazine Bioorthogonal Chemistry Driven by the Synthesis of Novel Tetrazines and Dienophiles. *Acc. Chem. Res.* **2018**, *51* (5), 1249–1259.
- (29) Novak, Z.; Kotschy, A. First Cross-Coupling Reactions on Tetrazines. *Org. Lett.* **2003**, *5* (19), 3495–3497.
- (30) Leconte, N.; Keromnes-Wuillaume, A.; Suzenet, F.; Guillaumet, G. Efficient Palladium-Catalyzed Synthesis of Unsymmetrical (Het)Aryltetrazines. *Synlett* **2007**, No. 2, 204–210.
- (31) Bender, A. M.; Chopko, T. C.; Bridges, T. M.; Lindsley, C. W. Preparation of Unsymmetrical 1,2,4,5-Tetrazines via a Mild Suzuki Cross-Coupling Reaction. *Org. Lett.* **2017**, *19* (20), 5693–5696.
- (32) Wiczorek, A.; Backup, T.; Wombacher, R. Rigid Tetrazine Fluorophore Conjugates with Fluorogenic Properties in the Inverse Electron Demand Diels–Alder Reaction. *Org. Biomol. Chem.* **2014**, *12* (24), 4177–4185.
- (33) Maji, S.; Sarkar, B.; Patra, S.; Fiedler, J.; Mobin, S. M.; Puranik, V. G. Metal-Induced Reductive Ring Opening of 1,2,4,5-Tetrazines: Three Resulting Coordination Alternatives, Including the New Non-Innocent 1,2-Diiminohydrazido(2–) Bridging Ligand System. *Inorg. Chem.* **2006**, *45* (3), 1316–1325.
- (34) Ruiz-Castillo, P.; Buchwald, S. L. Applications of Palladium-Catalyzed C–N Cross-Coupling Reactions. *Chem. Rev.* **2016**, *116* (19), 12564–12649.
- (35) Heravi, M. M.; Kheilkordi, Z.; Zadsirjan, V.; Heydari, M.; Malmir, M. Buchwald–Hartwig Reaction: An Overview. *J. Organomet. Chem.* **2018**, *861*, 17–104.
- (36) Quinton, C.; Alain-Rizzo, V.; Dumas-Verdes, C.; Clavier, G.; Vignau, L.; Audebert, P. Triphenylamine/Tetrazine Based π -Conjugated Systems as Molecular Donors for Organic Solar Cells. *New J. Chem.* **2015**, *39* (12), 9700–9713.
- (37) Wong, M. Y.; Zysman-Colman, E. Purely Organic Thermally Activated Delayed Fluorescence Materials for Organic Light-Emitting Diodes. *Adv. Mater.* **2017**, *29* (22), 1605444.
- (38) Yang, Z.; Mao, Z.; Xie, Z.; Zhang, Y.; Liu, S.; Zhao, J.; Xu, J.; Chi, Z.; Aldred, M. P. Recent Advances in Organic Thermally Activated Delayed Fluorescence Materials. *Chem. Soc. Rev.* **2017**, *46* (3), 915–1016.
- (39) Karon, K.; Lapkowski, M.; Dabulienė, A.; Tomkevičienė, A.; Kostiv, N.; Grazulevičius, J. V. Spectroelectrochemical Characterization of Conducting Polymers from Star-Shaped Carbazole-Triphenylamine Compounds. *Electrochim. Acta* **2015**, *154*, 119–127.
- (40) Pander, P.; Swist, A.; Zassowski, P.; Soloduch, J.; Lapkowski, M.; Data, P. Electrochemistry and Spectroelectrochemistry of Polymers Based on D–A–D and D–D–D Bis(N-Carbazolyl) Monomers, Effect of the Donor/Acceptor Core on Their Properties. *Electrochim. Acta* **2017**, *257*, 192–202.
- (41) Quinton, C.; Chi, S. H.; Dumas-Verdes, C.; Audebert, P.; Clavier, G.; Perry, J. W.; Alain-Rizzo, V. Novel S-Tetrazine-Based Dyes with Enhanced Two-Photon Absorption Cross-Section. *J. Mater. Chem. C* **2015**, *3* (32), 8351–8357.
- (42) Baba, M. Intersystem Crossing in the $1n\pi^*$ and $1\pi\pi^*$ States. *J. Phys. Chem. A* **2011**, *115* (34), 9514–9519.
- (43) Li, J.; Zhang, Q.; Nomura, H.; Miyazaki, H.; Adachi, C. Thermally Activated Delayed Fluorescence from $3n\pi^*$ to $1n\pi^*$ Up-Conversion and Its Application to Organic Light-Emitting Diodes. *Appl. Phys. Lett.* **2014**, *105*, 013301.
- (44) Carboni, R. A.; Lindsey, R. V. Reactions of Tetrazines with Unsaturated Compounds. A New Synthesis of Pyridazines. *J. Am. Chem. Soc.* **1959**, *81* (16), 4342–4346.
- (45) Sakya, S. M.; Strohmeyer, T. W.; Lang, S. A.; Lin, Y.-I. Preparation of Novel Tricyclic Diazo Carbapenems: Application of Inverse Electron Demand Diels–Alder Reactions of 3,6-Bis(Methylthio)-1,2,4,5-Tetrazine. *Tetrahedron Lett.* **1997**, *38* (34), 5913–5916.

- (46) Che, D.; Wegge, T.; Stubbs, M. T.; Seitz, G.; Meier, H.; Methfessel, C. Exo-2-(Pyridazin-4-Yl)-7-Azabicyclo[2.2.1]Heptanes: Syntheses and Nicotinic Acetylcholine Receptor Agonist Activity of Potent Pyridazine Analogues of (\pm)-Epibatidine. *J. Med. Chem.* **2001**, *44* (1), 47–57.
- (47) Sauer, J.; Heldmann, D. K.; Hetzenegger, J.; Krauthan, J.; Sichert, H.; Schuster, J. 1,2,4,5-Tetrazine: Synthesis and Reactivity in [4+2] Cycloadditions. *European J. Org. Chem.* **1998**, No. 12, 2885–2896.
- (48) Pander, P.; Swist, A.; Motyka, R.; Soloducho, J.; Dias, F. B.; Data, P. Thermally Activated Delayed Fluorescence with Narrow Emission Spectrum and Organic Room Temperature Phosphorescence by Controlling Spin-Orbit Coupling and Phosphorescence Lifetime of Metal-Free Organic Molecules. *J. Mater. Chem. C* **2018**, *6* (20), 5434–5443.
- (49) Pander, P.; Swist, A.; Soloducho, J.; Dias, F. B. Room Temperature Phosphorescence Lifetime and Spectrum Tuning of Substituted Thianthrenes. *Dye. Pigment.* **2017**, *142*, 315–322.
- (50) Baldo, M. A.; O'Brien, D. F.; You, Y.; Shoustikov, A.; Sibley, S.; Thompson, M. E.; Forrest, S. R. Highly Efficient Phosphorescent Emission from Organic Electroluminescent Devices. *Nature* **1998**, *395*, 151–154.
- (51) Liu, Y.; Zhan, G.; Liu, Z. W.; Bian, Z. Q.; Huang, C. H. Room-Temperature Phosphorescence from Purely Organic Materials. *Chinese Chem. Lett.* **2016**, *27* (8), 1231–1240.
- (52) Zhao, Q.; Huang, C.; Li, F. Phosphorescent Heavy-Metal Complexes for Bioimaging. *Chem. Soc. Rev.* **2011**, *40* (5), 2508–2524.
- (53) Lee, C. L.; Hwang, I. W.; Byeon, C. C.; Kim, B. H.; Greenham, N. C. Triplet Exciton and Polaron Dynamics in Phosphorescent Dye Blended Polymer Photovoltaic Devices. *Adv. Funct. Mater.* **2010**, *20* (17), 2945–2950.
- (54) Brandsma, L.; Verkruijsse, H. D. An Improved Synthesis of Cyclooctyne. *Synthesis (Stuttg.)*. **1978**, *4*, 290–290.
- (55) Sheldrick, G. M. SHELXS-97, Program for Crystal Structure Solution, University of Göttingen, Göttingen, Germany, **1997**.
- (56) Sheldrick, G. M. A short history of SHELX. *Acta Crystallogr., Sect. A: Found. Crystallogr.* **2008**, *64*, 112–122.
- (57) Farrugia, L. J. WinGX suite for small-molecule single-crystal crystallography. *J. Appl. Cryst.* **1999**, *32*, 837–838.